JOURNAL OF CATALYSIS 120, 465–472 (1989)

Structure of Ir/TiO_2 Catalysts

K. FOGER AND H. JAEGER

CSIRO, Division of Materials Science and Technology, Locked Bag 33, Clayton 3168, Victoria, Australia

Received May 4, 1989; revised August 7, 1989

The influence of oxidation–reduction treatments on the structure of Ir/TiO_2 (anatase–rutile mixtures) catalysts has been studied with TEM. The catalysts were further characterized with selective chemisorption of hydrogen and tested for hydrogenolysis of *n*-butane and 2,2-dimethylpropane. Upon oxidation at >670 K, Ir disappeared from the TiO_2 crystals and reappeared on reduction with a different shape and spatial distribution exclusively on the rutile crystals of the support. Compared to fresh catalysts, the oxidation–reduction treatment increased the rates of hydrogenolysis by factors of 15–30 for 2,2-dimethylpropane and by a factor of 2 for *n*-butane. It is suggested that the IrO_2 formed on oxidation migrated through the gas phase to the rutile crystals where it formed epitaxed monolayers.

1. INTRODUCTION

Titania has been investigated exhaustively as a support for transition metals (*1*) ever since Tauster *et al.* (*2*) reported the phenomena of strong metal–support interaction (SMSI) in 1978. The SMSI effect is observed with catalysts reduced above 600 K and has been attributed to surface modification of the metal particles by decoration with suboxide of titanium.

Titania has also been studied as a support for oxides (*3*) and sulfides (*4*) where it has shown the ability to change the structure of the dispersed phase.

In this study we report on Ir/TiO_2 catalysts and compare their properties with Ir/SiO_2 and Ir/Al_2O_3 catalysts. The catalysts were characterized with transmission electron microscopy (TEM), selective chemisorption of hydrogen, and hydrogenolysis of *n*-butane and 2,2-dimethylpropane.

2. EXPERIMENTAL

Two types of titania supports were employed: (i) a commercial titania (Degussa P25, consisting of 80% anatase and 20% rutile, surface area 50 m^2/g), subsequently referred to as P25, and (ii) an equimolar mixture of anatase (Tioxide, 120 m^2/g) and rutile (Tioxide, 24 m^2/g), subsequently referred to as TIOX. The other supports were SiO_2 (Aerosil, Degussa) and γ-Al_2O_3 (AKZO, 125 m^2/g).

Iridium catalysts were prepared by incipient wetness impregnation of the supports with chloriridic acid. The resulting slurries were dried in air at 400 K and reduced for 15 hr in flowing hydrogen at 520 K. The following catalysts were prepared: 5 wt% Ir/P25; 1 wt% Ir/P25; 1.7 wt% Ir/SiO_2; and 1 wt% Ir/SiO_2.

For the TEM study, samples were also prepared by direct vapour deposition of iridium metal onto the supports in a vacuum system. First, titania (P25 or TIOX) was spread on carbon-covered TEM grids made of gold. Then, iridium was vapour-deposited onto the TiO_2 layer on the grid (grid temperature, 298 K). The grids were mounted in a TEM environmental cell attachment and reduced in flowing hydrogen at 520 K.

Oxidation–reduction cycles of Ir/TiO_2 catalysts involved oxidation in flowing oxygen for 4 hr at 670–820 K, followed by reduction in flowing hydrogen for 15 hr at 520–770 K.

TEM micrographs were recorded using a JEOL 100CX microscope with an environ-

0021-9517/89 $3.00

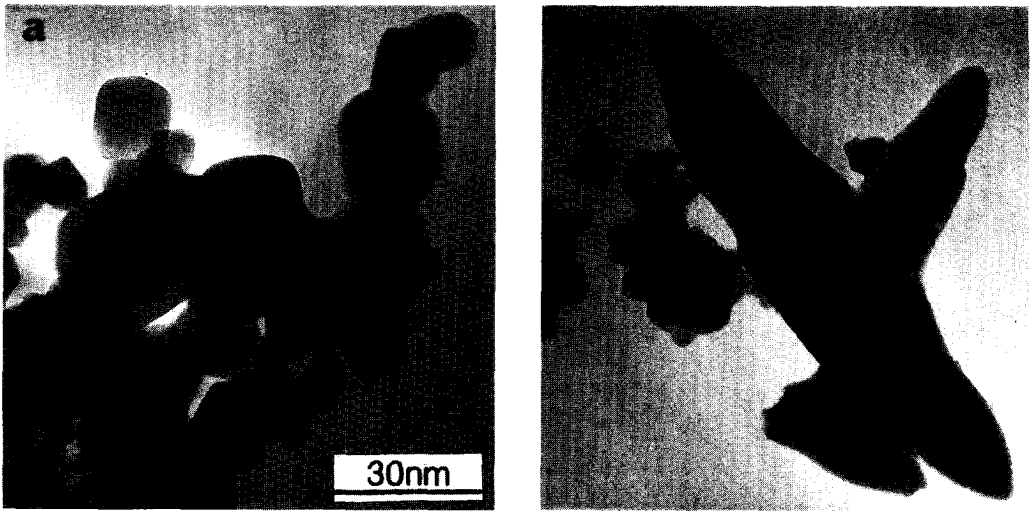

FIG. 1. TEM micrographs of titania supports, (a) P25 (Degussa) and (b) TIOX (Tioxide 120 m^2/g anatase + 24 m^2/g rutile).

mental cell attachment which permitted examination and oxidation–reduction treatment of specimens without exposure to air during transfer.

Hydrogen uptakes were measured at 298 K in a volumetric adsorption apparatus in the pressure range up to 50 kPa.

The hydrogenolysis of *n*-butane and 2,2-dimethylpropane was studied in a fixed-bed reactor operating under atmospheric pressure in differential mode. The feed gas consisted of a stream of hydrogen–hydrocarbon in a ratio 20/1. The products were analysed using an on-line gas chromatograph.

3. RESULTS

3.1. Structure Examination

3.1.1. Catalyst supports. Figures 1a and 1b show micrographs of P25 and TIOX. In P25 flattened rounded to rectangular particles approximately 10–50 nm in size were seen. P25 is a mixture of 80% anatase and 20% rutile as estimated from XRD traces, but it was not possible to differentiate between particles by TEM. The morphology was the same for all particles (Fig. 1a). Furthermore, SAD and darkfield imaging is unsuitable because of the small differences in lattice spacings of anatase and rutile. However, the absence of fault contrast and Moire fringes in individual particles indicated that there was no intergrowth between rutile and anatase. TEM examination prior to mixing of the separate components of TIOX established that the anatase component consisted of small (10 nm) rectangular or spherical particles and the rutile component of large banana-shaped particles, which often displayed angular or star-like intergrowth. These are readily differentiated in the mixture (Fig. 1b).

3.1.2. Fresh catalysts. In Ir on P25 (1 and 5 wt%) prepared by impregnation and reduction, metal particles ranged in size from 1 to 3 nm, and they were distributed evenly over all support particles (Figs. 2a and 2b). With vapour deposition it was possible to achieve higher densities of smaller Ir particles (<2 nm) distributed evenly over both anatase and rutile particles in P25 or TIOX (Figs. 2c and 2d). The arrow in Fig. 2d points at a rutile particle.

3.1.3. Oxidation 670–820 K, reduction 520–770 K. After oxidation, neither metal nor IrO_2 particles could be detected by TEM on either form of TiO_2 (Figs. 3a and

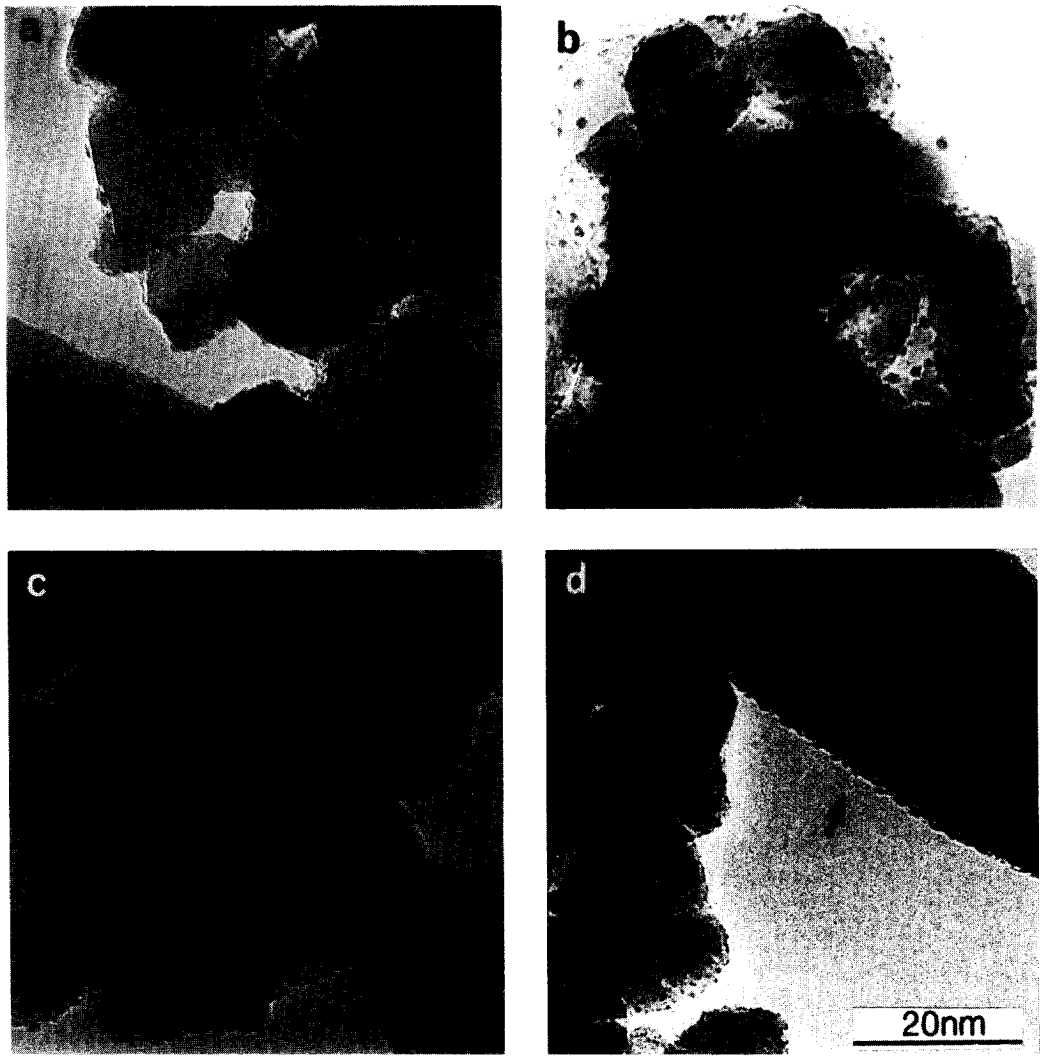

FIG. 2. TEM micrographs of fresh catalysts prepared by incipient wetness impregnation and reduction on P25, (a) 1 wt% Ir and (b) 5 wt% Ir; and by vacuum deposition (c) on P25 and (d) on TIOX.

3b) but chemical analysis showed that Ir had not been lost from the support. On SiO_2 and Al_2O_3, the metal also disappeared and needle-shaped IrO_2 crystals were observed instead (Fig. 3c).

On P25, after reduction, Ir particles could be detected with TEM only on some isolated substrate particles (Figs. 4a and 4b). These particles were otherwise indistinguishable from the rest of the support which was free from Ir. However, on TIOX, after reduction, Ir crystallites were detected on rutile particles only (Figs. 4c and 4d). Compared with that of the fresh catalysts the metal coverage after oxidation and reduction was higher on the rutile particles in TIOX and on the selected particles in P25 (cf. Figs. 2 and 4a, 4b, and 4c). Also, the metal particles were more plate-like and their concentration increased toward the edges of support particles.

On SiO_2 and Al_2O_3, after reduction, the IrO_2 crystals were converted to Ir polycrystalline aggregates (Fig. 3d).

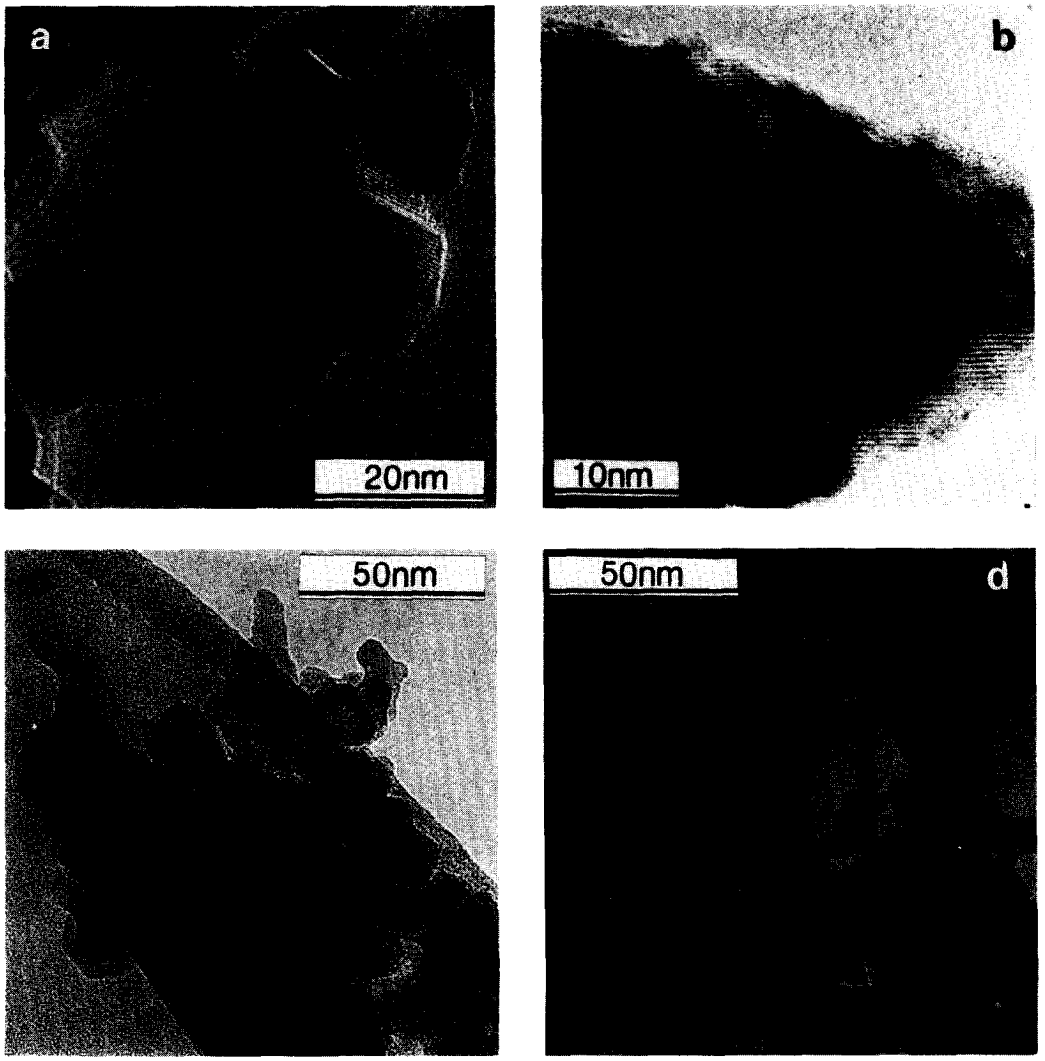

FIG. 3. TEM micrographs of catalysts oxidised in flowing O_2 > 720 K; (a) 5 wt% Ir on P25, (b) Ir on TIOX, (c) 1.7 wt% Ir on SiO_2, (d) 2.3 wt% Ir on Al_2O_3.

3.2. *Reaction Studies*

3.2.1. Hydrogen chemisorption. For Ir on P25 (1 and 5 wt%), dispersions of >95% were calculated from hydrogen uptakes assuming a stoichiometry of 1 H atom per Ir atom. Oxidation at 720 K and reduction at 520 K decreased the dispersions to 30–40%, but additional oxidation–reduction cycles did not decrease the dispersion any further. For Ir on SiO_2 and Al_2O_3, in contrast, the dispersions were significantly lower after only one oxidation–reduction cycle and were <5% after three cycles.

If fresh or oxidised Ir/TiO_2 catalysts were reduced above 570 K, dispersions calculated from hydrogen chemisorption were much lower than 30%, but TEM micrographs did not indicate sintering of iridium particles (Fig. 5a).

3.2.2. Hydrogenolysis. The hydrogenolysis results are summarized in Table 1. C_2 selectivities for *n*-butane and activities for hydrogenolysis of *n*-butane and 2,2-dimethylpropane of titania-supported catalysts agree well with those obtained previously for similar dispersions of Ir on SiO_2 and Al_2O_3 (*5, 6*), provided the titania-sup-

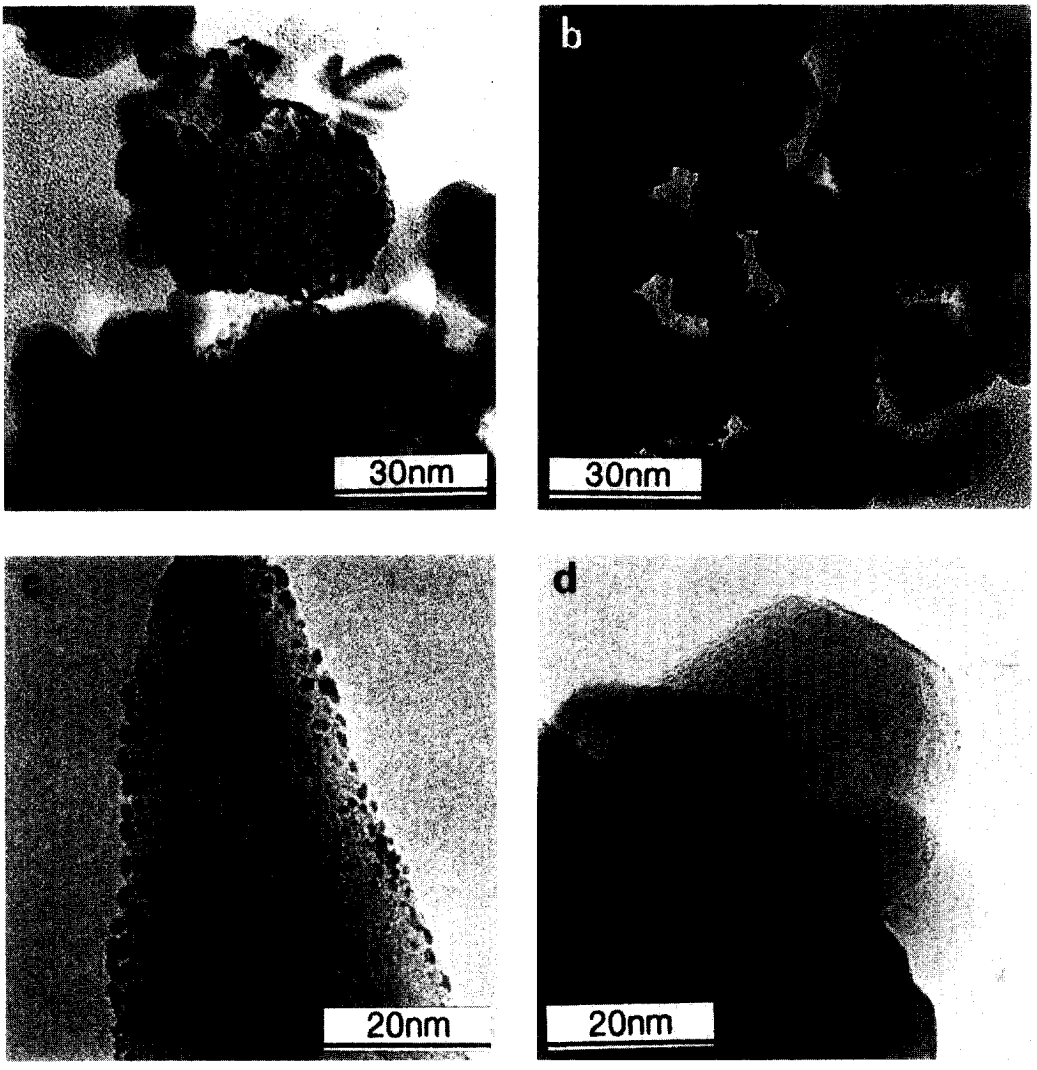

FIG. 4. TEM micrographs of catalysts oxidised at 720 K and reduced at 520 K; (a) 5% Ir on P25 prepared by impregnation and reduction; (b) Ir on P25; (c) Ir on TIOX, rutile component; and (d) Ir on TIOX, anatase particles. The catalysts depicted in (b), (c), and (d) were prepared by vacuum vapour deposition.

ported catalysts had not been exposed to oxidation at high temperature. After oxidation at >670 K and reduction at 520 K, their hydrogenolysis activity increased twofold for *n*-B, and 15 to 30 times for 22-DMPr. The ratios of hydrogenolysis activities for *n*-B and 22-DMPr, which indicate the preference for splitting bonds containing only primary and/or secondary carbon atoms and bonds containing quaternary carbons, are in the range 300–800 for fresh Ir/TiO_2 and for fresh or oxidised and reduced Ir/SiO_2 and Ir/Al_2O_3. However, the ratios are in the range 20–35 for Ir/TiO_2 after one oxidation and reduction cycle.

4. DISCUSSION

4.1. Structure of the Catalyst

Oxidation of Ir on titania above 670 K resulted in the disappearance of the small metal particles, but no iridium oxide phase was detected with either TEM or XRD.

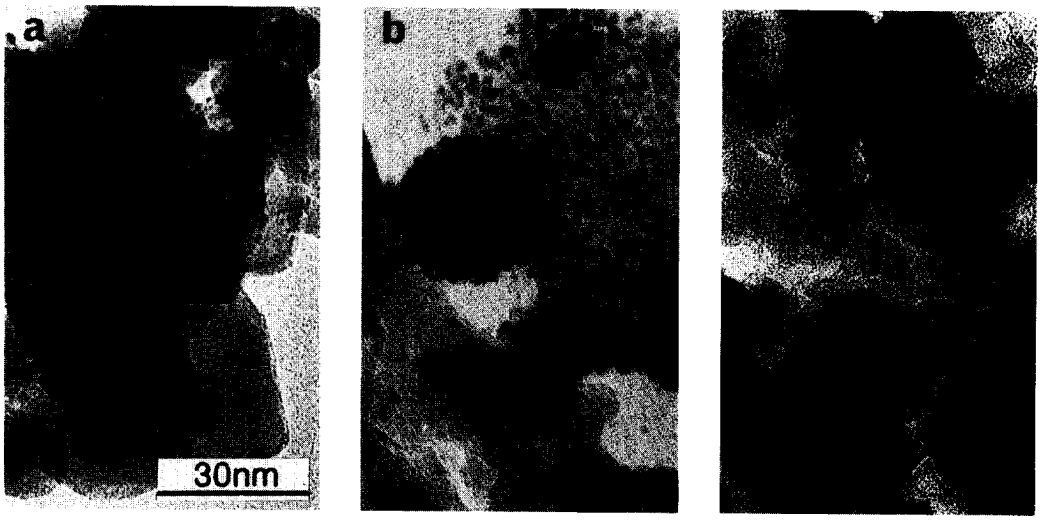

FIG. 5. TEM micrographs illustrating the influence of reduction temperature (T_r) on Ir particle size: (a) 5 wt% Ir on P25, T_r = 770 K; (b) 1.7 wt% Ir on SiO_2, T_r = 570 K; (c) 1.7 wt% Ir on SiO_2, T_r = 770 K.

Chemical analysis showed that Ir was not lost from the support during oxidation. In agreement with this, iridium particles reappeared on some TiO_2 grains upon reduction (e.g., Fig. 4). On TIOX, Ir particles were observed only on rutile crystals. Therefore, we infer that the support crystals in P25 which decorated with Ir particles upon reduction were also rutile.

In an earlier TEM and XRD study of the oxidation of Ir on silica and alumina (*7*), we observed that IrO_2 was formed above 670 K. Under static conditions, layers of IrO_2 encapsulated residual metal particles, but, under flow conditions, IrO_2 crystals grew initially out of metal particles, and later formed isolated larger crystals via vapour-phase transport. We believe that in the present case of titania, Ir was also oxidised to IrO_2 and then transported from anatase to rutile crystals either via surface migration or vapour-phase transport. Rutile (TiO_2) and iridia (IrO_2) have the same crystal structure (*9*) and very similar lattice parameters (rutile: a = 0.459 nm, c = 0.296 nm; iridia: a = 0.450 nm, c = 0.315 nm). Indeed, epitaxy has been demonstrated by Triggs *et al.* (*8*) for macroscopic crystals of IrO_2 formed by chemical vapour transport >1300 K onto polished (001), (100), and (110) surfaces of rutile. In the present work, we did not observe any evidence for IrO_2 crystals, even at edges of rutile particles where Ir crystals were formed preferentially upon reduction (Fig. 4). We therefore suggest that, under the milder conditions used here, IrO_2 epitaxed on exposed rutile surfaces in a layer-by-layer manner.

Comparison with earlier work (*7*) shows that Ir is much more resistant to sintering by thermal treatment in oxidising and reducing atmospheres on TiO_2 than on SiO_2 or Al_2O_3. For example, oxidation at 670 K followed by reduction at 520 K reduced the dispersion values (D) of Ir from above 95% to about 40% on TiO_2 (Table 1) and to less than 20% on SiO_2 and Al_2O_3 (*7*). Increasing the oxidation temperature and number of oxidation–reduction cycles further decreased the dispersion of Ir on SiO_2 and Al_2O_3, but on TiO_2 the dispersion remained unchanged. Increasing the reduction temperature from 570 K caused a sharp decrease in the dispersion value for Ir on TiO_2, but there was no fusion of metal particles to large aggregates (Fig. 5a). We therefore attribute the decrease in hydrogen chemisorption to the SMSI phenomenon,

TABLE 1

Hydrogenolysis Rates of *n*-Butane (*n*-B) and 2,2-Dimethylpropane (22-DMPr)

Catalysts	Treatment	H/Ir	d_{Ir} (nm)	Reaction rates at 473 K (molec. s^{-1} Ir_s^{-1})[a]		R^b	S_2^c
				n-Butane	2,2-Dimethylpropane		
5 wt% Ir on TiO^2 (P25)	None	0.95	1.3	2.1×10^{-2}	6.0×10^{-5}	350	0.75
	One cycle	0.35	3.5	4.0×10^{-2}	1.6×10^{-3}	25	0.55
	Three cycles	0.37	3.5	3.5×10^{-2}	1.5×10^{-3}	23	0.53
1 wt% Ir on P25	None	1.00	1.0	1.9×10^{-2}	6.5×10^{-5}	300	0.80
	One cycle	0.38	3.0	3.1×10^{-2}	9.8×10^{-4}	32	0.56
1.7% Ir on SiO_2	None	0.77	1.5	2.6×10^{-2}	3.5×10^{-5}	740	0.65
2.3% Ir on Al_2O_3[d]	None	0.75	1.5	1.5×10^{-2}	1.2×10^{-5}	1250	0.80
1 wt% Ir on SiO_2	One cycle	0.16	—	3.8×10^{-2}	5.0×10^{-5}	760	0.36

Note. Ratios (H/Ir) from hydrogen chemisorption and particle sizes (d_{Ir}) from TEM for Ir/TiO_2, Ir/SiO_2, and Ir/Al_2O_3 catalysts before and after oxidation–reduction treatment (an oxidation–reduction cycle consists of oxidation at 720 K followed by reduction at 520 K).

[a] Ir_s from H_2 uptake assuming H/Ir = 1.

[b] R = ratio (rate *n*-butane/rate 2,2-dimethylpropane).

[c] C_2 selectivity from *n*-butane.

[d] From Ref. (5).

where metal particles are partially or fully encapsulated by layers of titanium suboxide (*1*). This encapsulation appears to stabilize the metal particles against agglomeration at high reduction temperatures, since similar particles of Ir on SiO_2 or Al_2O_3 (*11*), resulting from reduction of thin metal halide layers under mild conditions, sinter rapidly at high reduction temperatures (cf. Figs. 5b and 5c).

4.2. Hydrogenolysis

On Ir/SiO_2, Ir/Al_2O_3, and fresh Ir/TiO_2 catalysts hydrogenolysis rates are 2 to 3 orders of magnitude larger for *n*-butane than for 2,2-dimethylpropane. Oxidation above 670 K and reduction below 520 K had no influence on hydrogenolysis for Ir/SiO_2, but for Ir/TiO_2 rates increased 15 to 30 times for 2,2-dimethylpropane and doubled for *n*-butane.

In the fresh Ir/TiO_2 catalysts most of the Ir is distributed evenly over all support particles whereas after oxidation–reduction, it is present only on rutile particles. However, earlier work (*12*) has shown that the hydrogenolysis behaviour of fresh Ir on either anatase or rutile is the same. The marked difference in reaction behaviour of Ir after oxidation–reduction, therefore indicates that Ir particles generated from thin iridium oxide films epitaxed on rutile differ in their surface structure from Ir particles resulting from other precursors.

Logan *et al.* (*13*) have shown with TEM that 5-nm Rh crystallites supported on P25 expose preferentially (111) facets. We assume Ir particles in alumina- and silica-supported and in fresh titania-supported catalysts will adopt a similar morphology. In this case, the reaction behaviour would be controlled by the particular distributions of atoms in high coordination number sites in (111) facets and in low coordination number sites at corners and edges.

In an earlier study (*5, 6*), it has been pos-

tulated that hydrogenolysis of hydrocarbons on Ir occurs by two distinct mechanisms:

(i) "C_2-unit" hydrogenolysis, which proceeds via fission of bonds involving primary and secondary carbon atoms. For this mechanism 1,2-adsorbed species with carbon–iridium double bonds have been postulated as intermediates (*11*), and the reaction predominates whenever the structure of the hydrocarbon allows the formation of such intermediates.

(ii) "Iso-unit" hydrogenolysis, which occurs whenever tertiary or quaternary carbon atoms are involved and proceeds via 1,3-adsorbed intermediates, bound to one (quasi-metallocycle) or two surface iridium atoms. This reaction is 2 to 3 orders of magnitude slower than "C_2-unit" hydrogenolysis as illustrated by the high values of R (ratio rate n-B/rate 2,2-DMPr) in Table 1.

Rates for "C_2-unit" and "Iso-unit" hydrogenolysis were not particularly sensitive to particle size changes (small variations do occur, but are probably within the error bars of measuring Ir_s and rate values), but internal bond splitting in n-butane (ethane formation) could be correlated with Ir crystallite size, with very small particles exhibiting the highest ethane selectivity (*5*). This is in agreement with a study of n-butane and 2,2-dimethylpropane over (111) and (110) surfaces of Ir (*14*), which found that: (i) ethane formation from n-butane increased with the number of Ir atoms of low coordination; and (ii) hydrogenolysis of 2,2-dimethylpropane was identical on (111) and (110) surfaces.

The current work, however, shows for Ir on rutile that high-temperature oxidation and low-temperature reduction increase the rate of hydrogenolysis of 2,2-dimethylpropane markedly, but have only a small effect on the rate of n-butane hydrogenolysis (values of R in Table 1 decrease significantly). Considering the previous findings, we believe that the active hydrogenolysis sites cannot be simply atoms in high coordination sites normally present on low index fcc planes but are more likely ensembles with a specific geometry (e.g., surface vacancies) which assist in the formation of a favourable reaction intermediate from 2,2-dimethylpropane.

REFERENCES

1. Bond, G. C., and Burch, R., "Catalysis" (Specialist Periodical Report), Vol. 6, p. 27. The Chemical Society, London, 1983.
2. Tauster, S. J., Fung, S. C., and Garten, R. L., *J. Amer. Chem. Soc.* **100,** 170 (1978).
3. Volta, J. C., *Stud. Surf. Sci. Catal.* **21,** 331 (1985).
4. Ng, K. Y. S., and Gulari, E., *J. Catal.* **95,** 33 (1985).
5. Foger, K., and Anderson, J. R., *J. Catal.* **59,** 325 (1979).
6. Foger, K., and Anderson, J. R., *J. Catal.* **64,** 448 (1980).
7. Foger, K., and Jaeger, H., *J. Catal.* **70,** 53 (1981).
8. Triggs, P., Georg, C. A., and Levy, F., *Mater. Res. Bull.* **17,** 671 (1982).
9. Rogers, D. B., Shannon, R. D., Sleight, A. W., and Gillson, J. L., *Inorg. Chem.* **8,** 841 (1969).
10. Dalmai-Imelik, G., Leclercq, C., and Maubert-Muguet, A., *J. Solid State Chem.* **16,** 129 (1976).
11. Foger, K., and Jaeger, H., *J. Catal.* **96,** 154 (1985).
12. Foger, K., *J. Catal.* **78,** 406 (1982).
13. Logan, D. A., Braunschweig, E. J., and Datye, A. K., *Langmuir* **4,** 827 (1988).
14. Engstrom, J. R., Goodman, D. W., and Weinberg, W. H., *J. Amer. Chem. Soc.* **110,** 8305 (1988).